International Journal for Innovative Engineering and Management Research
A Peer Revieved Open Access International Journal
www.ijiemr.org

COPY RIGHT

IJIEMR Transactions, online available on 23rd July 2017. Link :
http://www.ijiemr.org/downloads.php?vol=Volume-6&issue=ISSUE-5

Title: A Novel Compact Tri-Port Converter Fed SRM Drive With Flexible Energy Control Function Using Hybrid Fuzzy Logic Controller.

Volume 06, Issue 05, Page No: 2048 – 2062.

Paper Authors

*** SHAIK.KARIMULLA, MR. R. RAGHUNADHA SASTRY.**

* Department of Electrical & Electronics Engineering, NRI Institute of technology.

USE THIS BARCODE TO ACCESS YOUR ONLINE PAPER

To Secure Your Paper As Per UGC Guidelines We Are Providing A Electronic Bar Code

International Journal for Innovative Engineering and Management Research
A Peer Revieved Open Access International Journal
www.ijiemr.org

A NOVEL COMPACT TRI-PORT CONVERTER FED SRM DRIVE WITH FLEXIBLE ENERGY CONTROL FUNCTION USING HYBRID FUZZY LOGIC CONTROLLER

***SHAIK.KARIMULLA, **MR. R. RAGHUNADHA SASTRY**

*PG Scholar, Department of Electrical & Electronics Engineering, NRI Institute of technology, Andhra Pradesh, India.

.**Associative Professor, Department of Electrical & Electronics Engineering, NRI Institute of technology, Andhra Pradesh, India.

karimullah143@gmail.com raghunath.rrs@gmail.com

ABSTRACT:

This project presents the use of Hybrid fuzzy logic control (FLC) for switched reluctance motor (SRM) speed. Switched Reluctance Motors (SRM) has a wide range of industrial applications because of their advantages over conventional AC/DC Drives. This is due to simple construction, ruggedness and inexpensive manufacturing potential. Various methods have used and applied to control SRM speed generally, the PV-fed EV has a similar structure to the hybrid electrical vehicle, whose internal combustion engine (ICE) is replaced by the PV panel. The PV has different characteristics to ICEs, the maximum power point tracking (MPPT) and solar energy utilization are the unique factors for the PV-fed EVs. In order to achieve low cost and flexible energy flow modes, a low cost tri-port converter is implemented. Proposed Tri-port converter is used to control the energy flow between the PV panel, battery and SRM. When the PV panel directly charges the battery, a multi-section charging control strategy is used to optimize energy utilization. The Hybrid FLC performs a PI-like control strategy, giving the current reference variation based on speed error and its change. The performance of the drive system is evaluated through MATLAB/SIMULINK software.

Key Words: Electric vehicles, photovoltaic's (PV), power flow control, switched reluctance motors (SRMs), tri-port converter, Fuzzy Logic Controller, Hybrid fuzzy logic controller**.**

I. INTRODUCTION

Switched Reluctance Motor (SRM) drives have been used for many years in applications, where simplicity of construction was primary important [1]. An SRM is a rotating electric motor, where both stator and rotor have salient poles [2]. The stator winding comprises a set of coils, each of which is wound on one pole. The rotor is made from laminated in order to minimize the eddy current losses [3]. The rotor tries to get to a position of minimum reluctance by aligning itself with the stator magnetic field when the stator winding are excited [4]. Due to its attractive features of high power density, high efficiency and low maintenance cost, SRM is widely used in high performance servo applications, such as aerospace, industrial and robotics [5-10]. SRM cannot be run directly from the supply. It can be run only when the motor is integrated with a power converter, controller and rotor position sensor. Many researchers have been reported on the performance simulation of SRM with experimental validation for different control strategies such a feedback linearization control,

International Journal for Innovative Engineering and Management Research
A Peer Revieved Open Access International Journal
www.ijiemr.org

variable structure control, fuzzy logic control and four quadrant operation of SRM [11-15]. None of these have focused exclusively on fast tracking capability, less steady state error and robust to load disturbance during steady state and transient conditions. Hence, it is necessary to design a hybrid fuzzy controller for SRM to get the optimum performance in the presence of the parameters variations and load disturbances. This study proposes a hybrid fuzzy controller where in discrete PI and fuzzy logic control algorithms are combined to get the desired performance of SRM. This controller employs only with the speed error and changes in speed error and produces an equivalent control term. The designed hybrid fuzzy controller improves system performance in transient and steady state.

Generally, the PV-fed EV has a similar structure to the hybrid electrical vehicle, whose internal combustion engine (ICE) is replaced by the PV panel. The PV-fed EV system is illustrated in Fig.1. Its key components include an off-board charging station, a PV, batteries and power converters. In order to decrease the energy conversion processes, one approach is to redesign the motor to include some on-board charging functions. For instance, paper designs a 20-kW split-phase PM motor for EV charging, but it suffers from high harmonic contents in the back electromotive force (EMF). Another solution is based on a traditional SRM. Paper achieves on-board charging and power factor correction in a 2.3-kW SRM by employing machine windings as the input filter inductor. The concept of modular structure of driving topology is proposed in paper. Based on intelligent power modules (IPM), a four-phase half bridge converter is employed to achieve driving and grid-charging. Although modularization supports mass production, the use of half/full bridge topology reduces the system reliability (e.g. shoot-through issues). Paper develops a simple topology for plug-in hybrid electrical vehicle (HEV) that supports flexible energy flow. But for grid charging, the grid should be connected to the generator rectifier that increases the energy conversion process and decreases the charging efficiency. Nonetheless, an effective topology and control strategy for PV-fed EVs is not yet developed. Because the PV has different characteristics to ICEs, the maximum power point tracking (MPPT) and solar energy utilization are the unique factors for the PV-fed EVs.

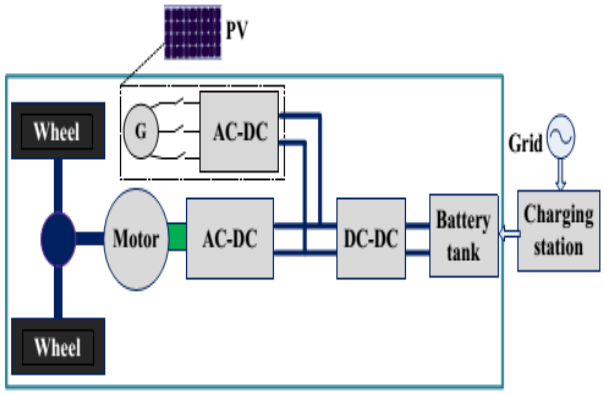

Fig.1 PV-fed hybrid electrical vehicle

II. TOPOLOGY AND OPERATIONAL MODES

A. Proposed topology and working modes

The proposed Tri-port topology has three energy terminals, PV, battery and SRM. They are linked by a power converter which consists of four switching devices (S0~S3), four diodes (D0~D3) and two relays, as shown in Fig.2 [26]. By controlling relays J1 and J2, the six operation modes are supported, as shown in Fig. 3; the corresponding relay actions are illustrated in Table I. In mode 1, PV is the energy source to drive the SRM and to charge the battery. In mode 2, the PV and battery are both the energy sources to drive the SRM. In mode 3, the PV is the source and the battery is idle. In mode 4, the battery is the driving source and the PV is idle. In mode 5, the battery is charged by a single-phase grid

International Journal for Innovative Engineering and Management Research
A Peer Revieved Open Access International Journal
www.ijiemr.org

while both the PV and SRM are idle. In mode 6, the battery is charged by the PV and the SRM is idle.

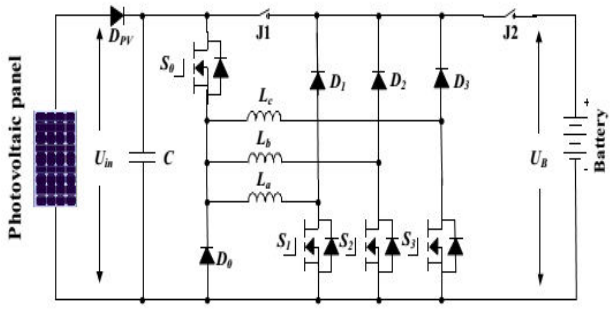

Fig.2. The proposed Tri-port topology for PV-powered SRM drive

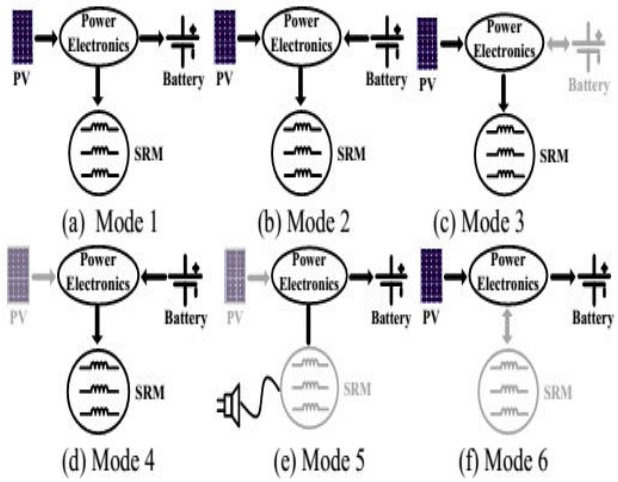

Fig.3. Six operation modes of the proposed Tri-port topology

TABLE 1 J1 and J2 Actions under Different Modes

Mode	J1 and J2
1	J1 turn-off; J2 turn-on
2	J1 and J2 turn-on
3	J1 turn-on; J2 turn-off
4	J1 and J2 turn-on
5	J1 and J2 turn-on
6	J1 turn-off; J2 turn-on

B. Driving modes

Operating modes 1~4 are the driving modes to provide traction drive to the vehicle.

(1) Mode 1

At light loads of operation, the energy generated from the PV is more than the SRM needed; the system operates in mode 1. The corresponding operation circuit is shown in Fig.4 (a), in which relay J1 turns off and relay J2 turns on. The PV panel energy feed the energy to SRM and charge the battery; so in this mode, the battery is charged in EV operation condition.

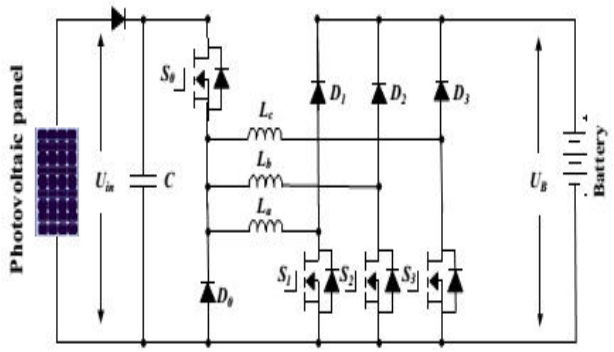

(a) Operation circuit under mode 1

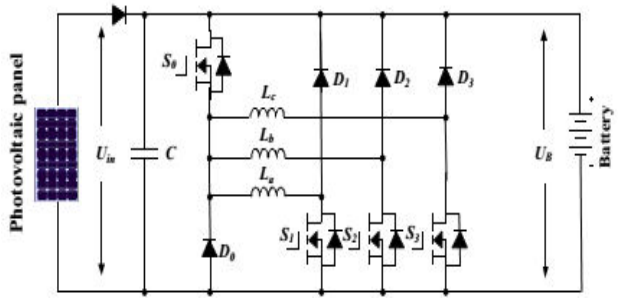

(b) Operation circuit under mode 2

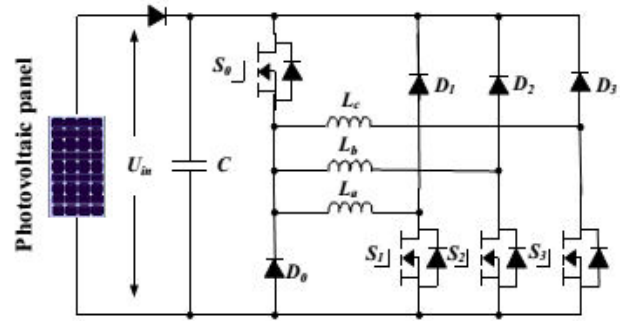

(c) Operation circuit under mode 3

International Journal for Innovative Engineering and Management Research
A Peer Revieved Open Access International Journal
www.ijiemr.org

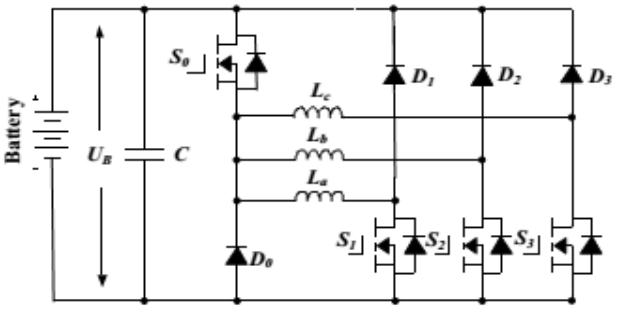

(d) Operation circuit under mode 4

Fig.4 The equivalent circuits under driving modes

(2) Mode 2

When the SRM operates in heavy load such as uphill driving or acceleration, both the PV panel and battery supply power to the SRM. The corresponding operation circuit is shown in Fig.4 (b), in which relay J1 and J2 are turned on.

(3) Mode 3

When the battery is out of power, the PV panel is the only energy source to drive the vehicle. The corresponding circuit is shown in Fig.4 (c). J1 turns on and J2 turns off.

(4) Mode 4

When the PV cannot generate electricity due to low solar irradiation, the battery supplies power to the SRM. The corresponding topology is illustrated in Fig.4 (d). In this mode, relay J1 and J2 are both conducting.

C. Battery charging modes

Operating modes 5 and 6 are the battery charging modes.

(5) Mode 5

When PV cannot generate electricity, an external power source is needed to charge the battery, such as AC grid. The corresponding circuit is shown in Fig.5 (a). J1 and J2 turns on. Point A is central tapped of phase windings that can be easily achieved without changing the motor structure. One of the three phase windings is split and its midpoint is pulled out, as shown in Fig.5 (a). Phase windings La1 and La2 are employed as input filter inductors. These inductors are part of the drive circuit to form an AC-DC rectifier for grid charging.

(6) Mode 6

When the EV is parked under the sun, the PV can charge the battery. J1 turns off; J2 turns on. The corresponding charging circuit is shown in Fig.5 (b).

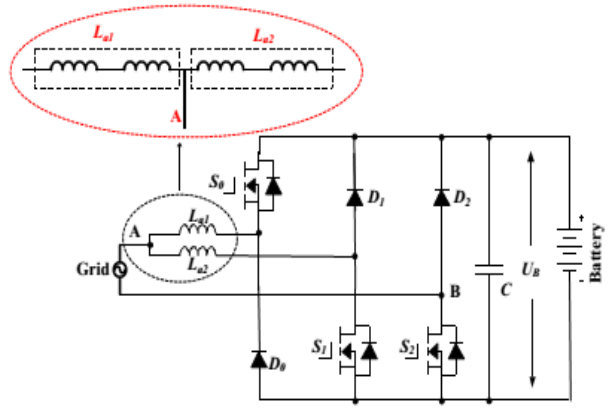

(a) Grid charging mode

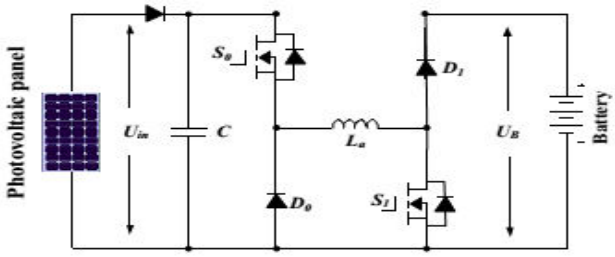

(b) PV source charging mode

Fig.5 Equivalent circuits of charging condition modes

III. Control Strategy under Different Modes

In order to make the best use of solar energy for driving the EV, a control strategy under different modes is designed.

B. Single source driving mode

According to the difference in the power sources, there are PV-driving; battery-driving and PV and battery parallel fed source. In a heavy load condition, the PV power cannot support the EV, mode 2 can be adopted to support enough energy and make full use of solar energy. Fig.6 (a) shows the equivalent

International Journal for Innovative Engineering and Management Research
A Peer Revieved Open Access International Journal
www.ijiemr.org

power source; the corresponding PV panel working points is illustrated in Fig.6 (b). Because the PV is paralleled with the battery, the PV panel voltage is clamped to the battery voltage UB. In mode 2, there are three working states: winding excitation, energy recycling and freewheeling states, as shown in Fig.7. Modes 3 and 4 have similar working states to mode 2. The difference is that the PV is the only source in mode 3 while the battery is the only source in mode 4.

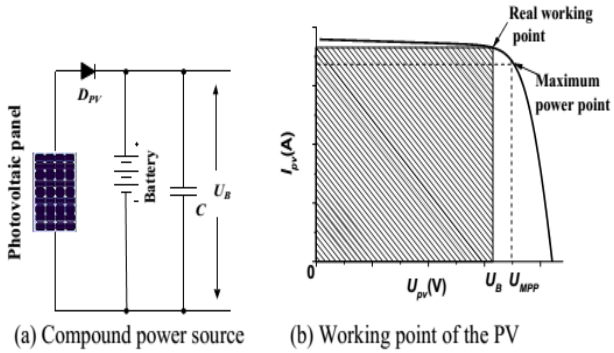

Fig.6 Power supply at mode 2

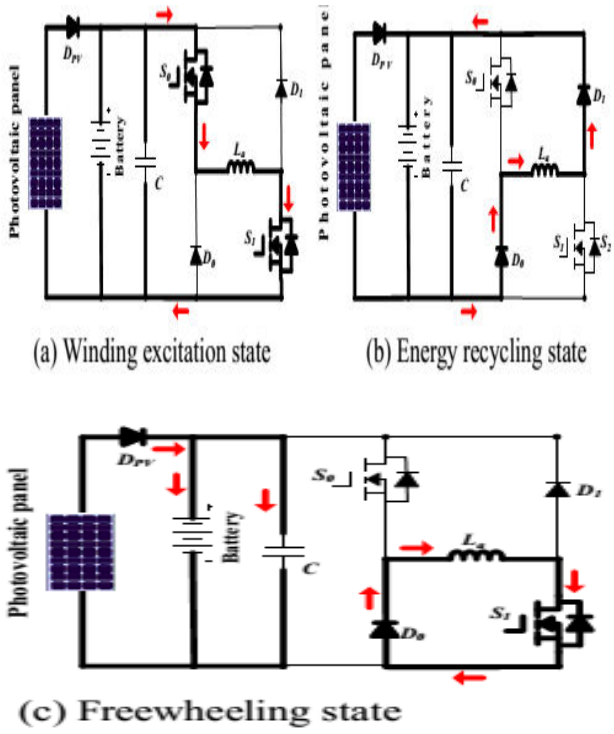

Fig.7 Working states at mode 2

Neglecting the voltage drop across the power switches and diodes, the phase voltage is given by

$$U_{in} = R_k i_k + \frac{d\psi(i_k,\theta_r)}{dt}$$
$$= R_k i_k + L_k \frac{di_k}{dt} + i_k \omega_r \frac{dL_k}{d\theta_r}, \quad k = a,b,c \tag{1}$$

where U_{in} is the DC-link voltage, k is phase a, b, or c, R_k is the phase resistance, i_k is the phase current, L_k is the phase inductance, θr is the rotor position, $\psi(i_k, \theta_r)$ is the phase flux linkage depending on the phase current and rotor position, and ωr is the angular speed. The third term in Eq.1 is the back electromotive force (EMF) voltage given by

$$e_k = i_k \omega_r \frac{dL_k}{d\theta_r} \tag{2}$$

Hence, the phase voltage is found by

$$U_k = R_k i_k + L_k \frac{di_k}{dt} + e_k \tag{3}$$

In the excitation region, turning on S0 and S1 will induce a current in phase a winding, as show in Fig.7 (a). Phase a winding is subjected to the positive DC bus voltage.

$$+U_{in} = R_k i_k + L_k \frac{di_k}{dt} + e_k \tag{4}$$

When S0 is off and S1 is on, the phase current is in a freewheeling state in a zero voltage loop, as shown in Fig.3.7(c), the phase voltage is zero.

$$0 = R_k i_k + L_k \frac{di_k}{dt} + e_k \tag{5}$$

In the demagnetization region, S0 and S1 are both turned off, and the phase current will flow back to the power supply, as show in Fig.7(b). In this state, the phase winding is subjected to the negative DC bus voltage, and the phase voltage is

International Journal for Innovative Engineering and Management Research
A Peer Revieved Open Access International Journal
www.ijiemr.org

$$-U_{in} = R_k i_k + L_k \frac{di_k}{dt} + e_k \quad (6)$$

In single source driving mode, the voltage-PWM control is employed as the basic scheme, as illustrated in Fig.8. According to the given speed ω*, the voltage-PWM control is activated at speed control.

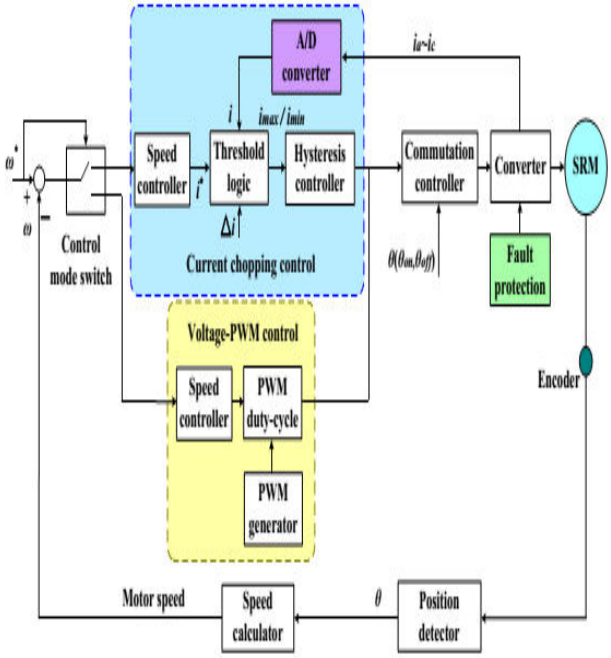

Fig.8 SRM control strategy under single source driving mode

B. Driving-charging hybrid control strategy

In the driving-charging hybrid control, the PV is the driving source and the battery is charged by the freewheeling current, as illustrated in drive mode 1. There are two control objectives: maximum power point tracking (MPPT) of the PV panel and speed control of the SRM.

The dual-source condition is switched from a PV-driving mode. Firstly, the motor speed is controlled at a given speed in mode 3. Then, J2 is tuned on and J1 is off to switch to mode 1. By controlling the turn-off angle, the maximum power of PV panel can be tracked.

There are three steady working states for the dual-source mode (mode 1), as shown in Fig.9. In Fig.9 (a), S0 and S1 conduct, the PV panel charges the SRM winding to drive the motor; In Fig.9 (b), S0 and S1 turn off; and the battery is charged with freewheeling current of the phase winding. Fig.9 (c) shows a freewheeling state.

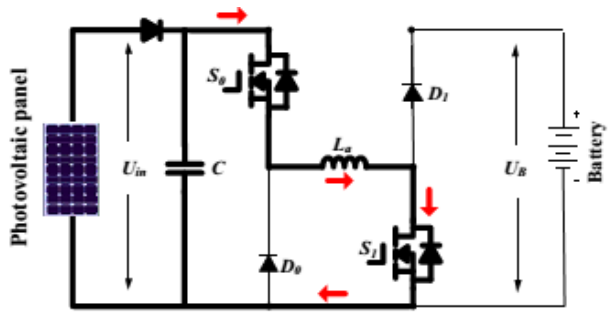

(a) Winding exciting state

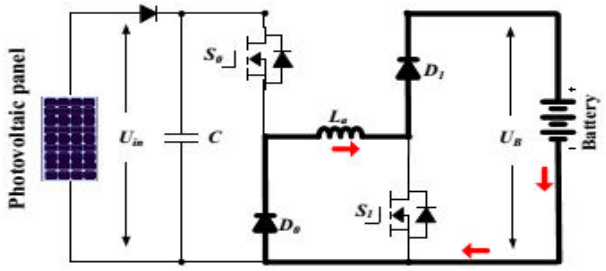

(b) Battery charging state

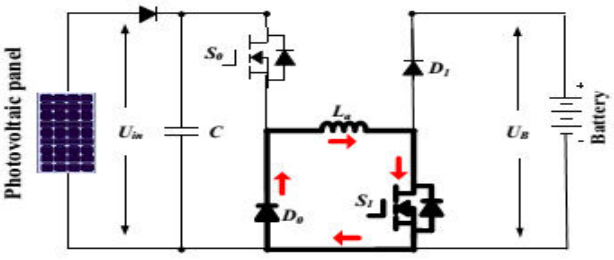

(c) Freewheeling state

Fig.9 Mode 1 working states

Fig.10 is the control strategy under driving-charging mode. In Fig.10, θon is the turn on angle of SRM; θoff is the turn-off angle of SRM. By adjusting turn-on angle, the speed

International Journal for Innovative Engineering and Management Research
A Peer Revieved Open Access International Journal
www.ijiemr.org

of SRM can be controlled; the maximum power point tracking of PV panel can be achieved by adjusting turn-off angle, which can control the charging current to the battery.

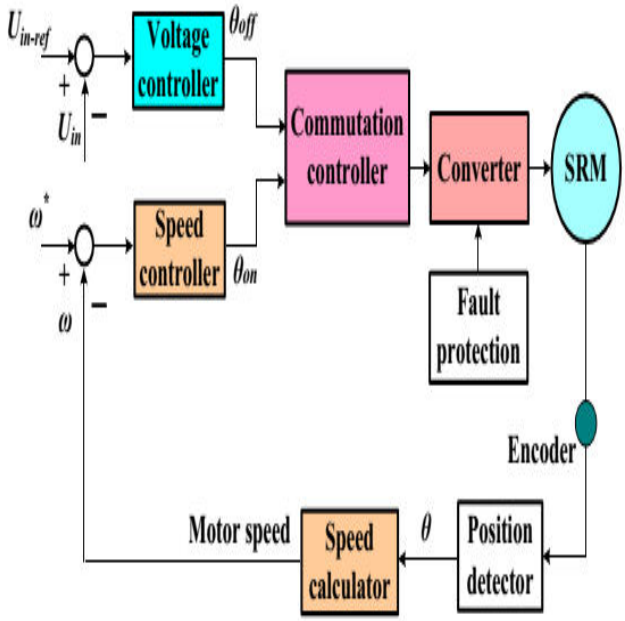

Fig.10. Control strategy under driving-charging mode (mode 1)

C. Grid-charging control strategy

The proposed topology also supports the single-phase grid charging. There are four basic charging states and S0 is always turned off. When the grid instantaneous voltage is over zero, the two working states are presented in Fig.11 (a) and (b). In Fig.11 (a), S1 and S2 conduct, the grid voltage charges the phase winding La2, the corresponding equation can be expressed as Eq.7; In Fig.11 (b), S1 turns off and S2 conducts, the grid is connected in series with phase winding to charges the battery, the corresponding equation can be expressed as Eq.8.

$$U_{grid} = L_{a2} \cdot \frac{di_{grid}}{dt} \tag{7}$$

$$U_B - U_{grid} = L_{a2} \cdot \frac{di_{grid}}{dt} \tag{8}$$

When the grid instantaneous voltage is below zero, the two working states are

presented in Fig.11 (c) and (d). In Fig.11(c), S1 and S2 conduct, the grid voltage charges the phase winding La1 and La2, the corresponding equation can be expressed as Eq. (9); In Fig.11(d), S1 keeps conducing and S2 turns off, the grid is connected in series with phase winding La1 and La2 to charges the battery, the corresponding equation can be expressed as Eq.10.

$$U_{grid} = \frac{L_{a1} + L_{a2}}{L_{a1} \cdot L_{a2}} \cdot \frac{di_{grid}}{dt} \tag{9}$$

$$-U_B - U_{grid} = \frac{L_{a1} + L_{a2}}{L_{a1} \cdot L_{a2}} \cdot \frac{di_{grid}}{dt} \tag{10}$$

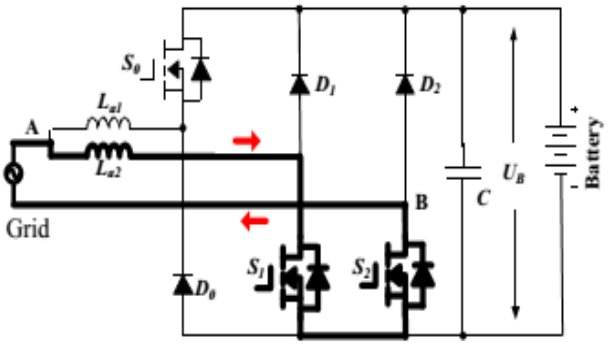

(a) Grid charging state 1 (Ugrid>0)

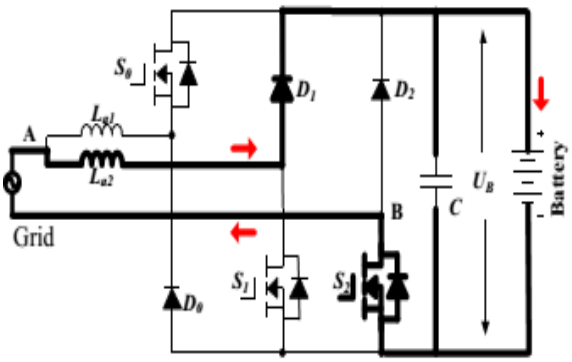

(b) Grid charging state 2 (Ugrid>0)

International Journal for Innovative Engineering and Management Research
A Peer Revieved Open Access International Journal
www.ijiemr.org

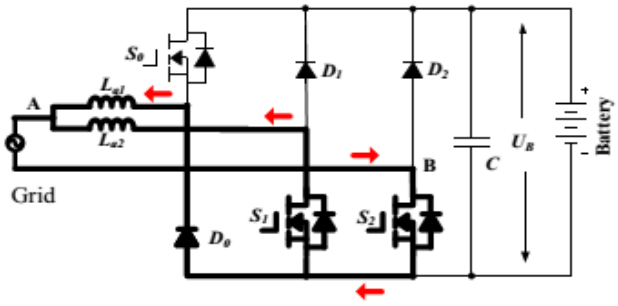

(c) Grid charging state 3 (Ugrid<0)

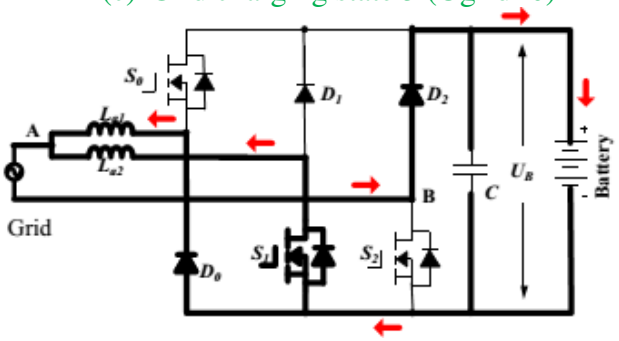

(d) Grid charging state 4 (Ugrid<0)

Fig.3.11 Mode 5 charging states

In Fig.12, Ugrid is the grid voltage; by the phase lock loop (PLL), the phase information can be got; Iref_grid is the given amplitude of the grid current. Combining sinθ and Iref_grid, the instantaneous grid current reference iref_grid can be calculated. In this mode, when Ugrid> 0, the inductance is La2; when Ugrid< 0, the inductance is paralleled La1 and La2; in order to adopt the change in the inductance, hysteresis control is employed to realize grid current regulation. Furthermore, hysteresis control has excellent loop performance, global stability and small phase lag that makes grid connected control stable.

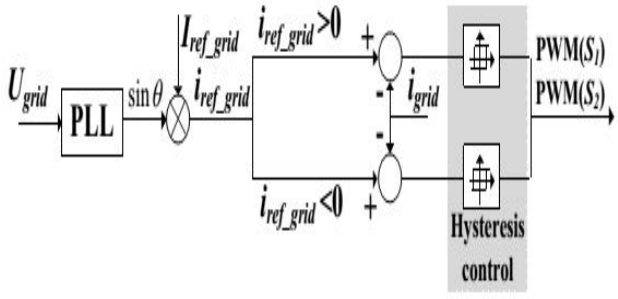

Fig.12 Grid-connected charging control (Mode5)

D. PV-fed charging control strategy

In this mode, the PV panel charges the battery directly by the driving topology. The phase windings are employed as inductor; and the driving topology can be functioned as interleaved Buck boost charging topology. For one phase, there are two states, as shown in Fig.13 (a) and (b). When S0 and S1 turn on, the PV panel charges phase inductance; when S0 and S1 turns off, the phase inductance discharges energy to battery. According to the state-of-charging (SoC), there are three stages to make full use of solar energy and maintain battery healthy condition, as illustrated in Fig.13 (c). During stage 1, the corresponding battery SoC is in 0~SoC1, the battery is in extremely lack energy condition, the MPPT control strategy is employed to make full use of solar energy. During stage 2, the corresponding battery SoC is in SoC1~ SoC2, the constant voltage control is adapted to charging the battery. During stage 3, the corresponding battery SoC is in SoC2~1, the micro current charging is adapted. In order to simplify the control strategy, constant voltage is employed in PV panel MPPT control.

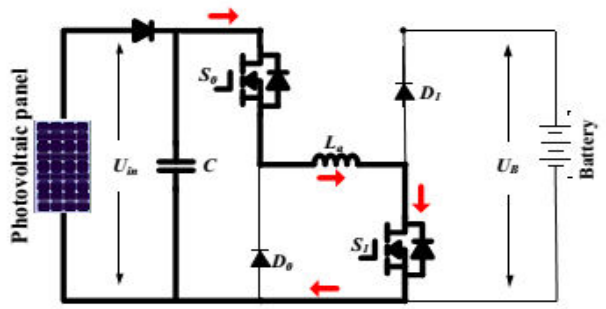

(a) Phase inductance charging

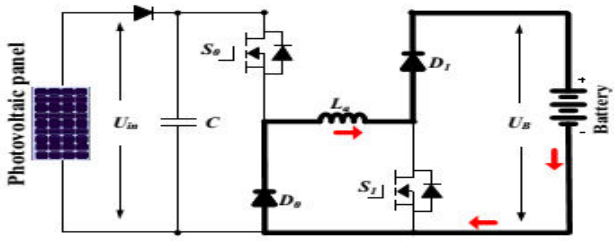

(b) Battery charging

International Journal for Innovative Engineering and Management Research
A Peer Revieved Open Access International Journal
www.ijiemr.org

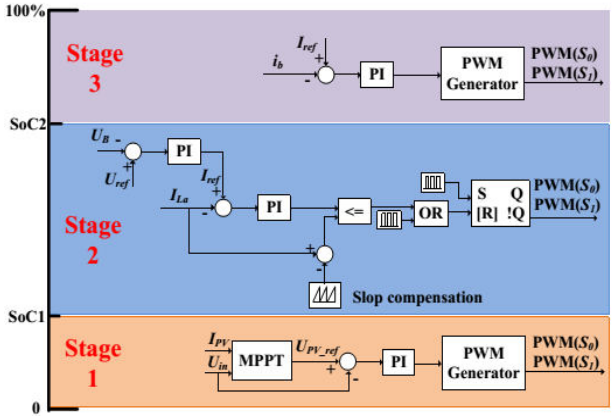

(c) Charging control strategy.

Fig.13 Mode 6 charging states and control strategy.

IV. DESIGN OF A FUZZY CONTROLLER

The difficulty regarding the PI controller gain is the fine tuning of the controller so as to achieve the optimal operation of the task. The major drawback of the PI controller is faced when the process is nonlinear and also when the system is having oscillations. Considering all these facts, a fuzzy logic controller was implemented. A fuzzy controller can work in linear as well as in nonlinear design parameters. FL requires some numerical parameters in order to operate such as what is considered significant error and significant rate-of-change-of error, but exact values of these numbers are usually not critical unless very responsive performance is required in which case empirical tuning would determine them.

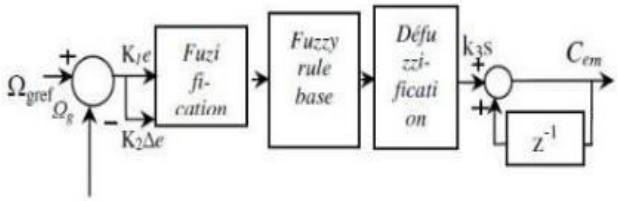

Fig.14 Fuzzy Logic Controller

FL requires some numerical parameters in order to operate such as what is considered significant error and significant rate-of-change-of-error, but exact values of these numbers are usually not critical unless very responsive performance is required in which case empirical tuning would determine them. For example, a simple temperature control system could use a single temperature feedback sensor whose data is subtracted from the command signal to compute "error" and then time-differentiated to yield the error slope or rate-of change-of-error, hereafter called "error-dot".

V. HYBRID FUZZY CONTROLLER

The objective of the hybrid controller is to utilize the best attributes of the PI and fuzzy logic controllers to provide a controller which will produce better response than either the PI or the fuzzy controller. There are two major differences between the tracking ability of the conventional PI controller and the fuzzy logic controller. Both the PI and fuzzy controller produce reasonably good tracking for steady-state or slowly varying operating conditions. However, when there is a step change in any of the operating conditions, such as may occur in the set point or load, the PI controller tends to exhibit some overshoot or oscillations. The fuzzy controller reduces both the overshoot and extent of oscillations under the same operating conditions. Although the fuzzy controller has a slower response by itself, it reduces both the overshoot and extent of oscillations under the same operating conditions. The desire is that, by combining the two controllers, one can get the quick response of the PI controller while eliminating the overshoot possibly associated with it. Switching Control Strategy the switching between the two controllers needs a reliable basis for determining which controller would be more effective.

The answer could be derived by looking at the advantages of each controller. Both controllers yield good responses to steady-state or slowly changing conditions. To take

International Journal for Innovative Engineering and Management Research
A Peer Revieved Open Access International Journal
www.ijiemr.org

advantage of the rapid response of the PI controller, one needs to keep the system responding under the PI controller for a majority of the time, and use the fuzzy controller only when the system behavior is oscillatory or tends to overshoot. Thus, after designing the best stand-alone PI and fuzzy controllers, one needs to develop a mechanism for switching from the PI to the fuzzy controllers, based on the following two conditions:

- Switch when oscillations are detected;
- Switch when overshoot is detected.

The switching strategy is then simply based on the following conditions: IF the system has an oscillatory behavior then fuzzy controller is activated, Otherwise PI controller is operated. IF the system has an overshoot then fuzzy controller is activated, Otherwise PI controller is operated. The system under study is considered as having an overshoot when the error is zero and the rate of change in error is any other value than zero. The system is considered oscillatory when the sum of the absolute values of the error taken over time does not equal the absolute values of the sum of the error over the same period of time. Since the system is expected to overshoot during oscillatory behavior, the only switching criterion that needs to be considered is overshoot. However, in practice, it is more convenient to directly implement the control signal according to the control actions delivered by the controller. Consequently, the fuzzy controller can be designed so that normal behavior (no oscillations or overshoot) results in a null fuzzy action as shown in Fig.4. Accordingly, the switching between the two controllers reduces to using PI if the fuzzy has null value; otherwise, the fuzzy output is used. In particular, the fuzzy controller can be designed so that a normal behavior.

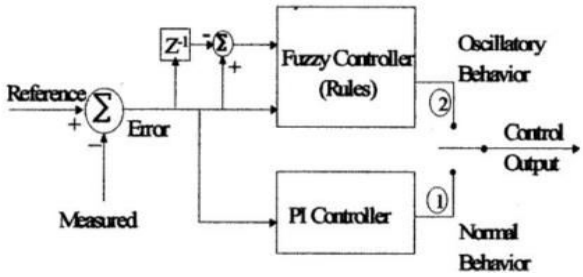

Fig.15 Structure of switching strategy results in a null fuzzy action.

VI. MATLAB/SIMULATION RESULTS

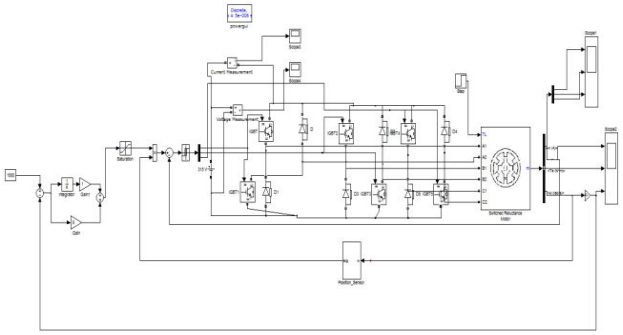

Fig.16 SRM drive model diagram

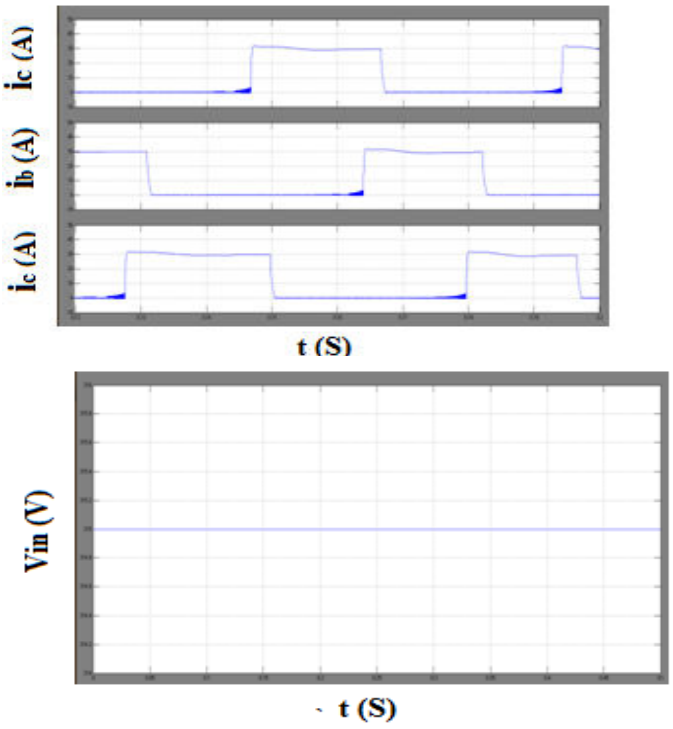

International Journal for Innovative Engineering and Management Research
A Peer Revieved Open Access International Journal
www.ijiemr.org

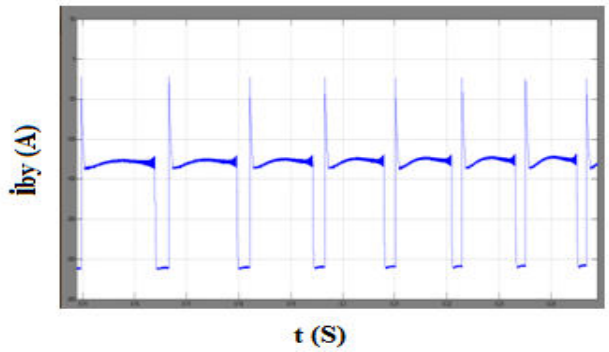

(a) Simulation results of driving-charging mode (mode 1)

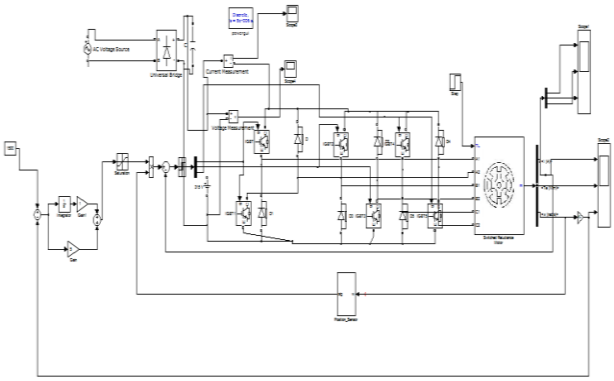

Fig.16 SRM drive model diagram

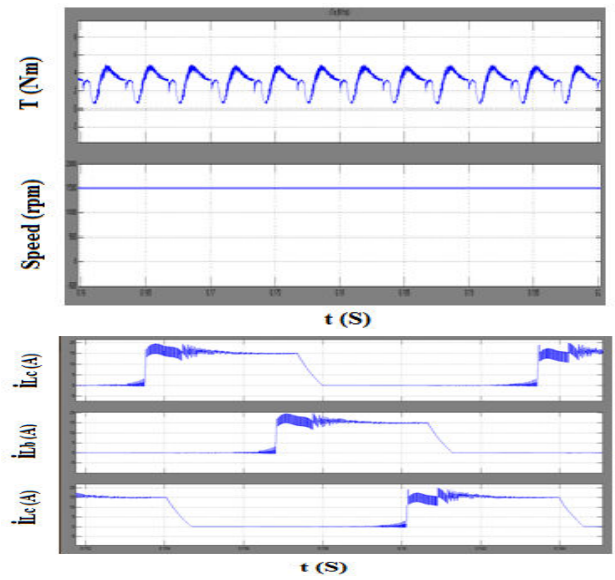

(b) Simulation results of single source driving mode (modes 3 and 4)

Fig.17 Simulation results for driving conditions at modes 1, 3 and 4.

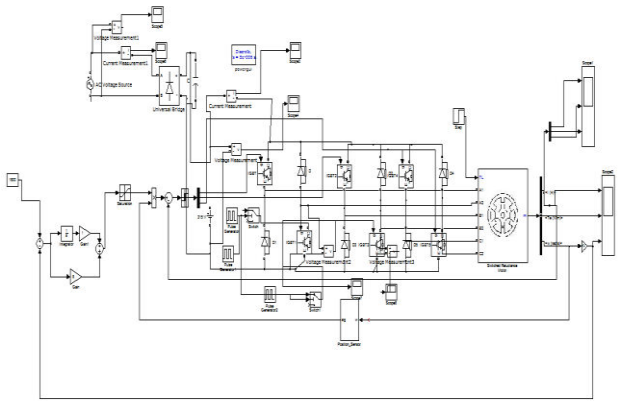

Fig.18 SRM drive model diagram

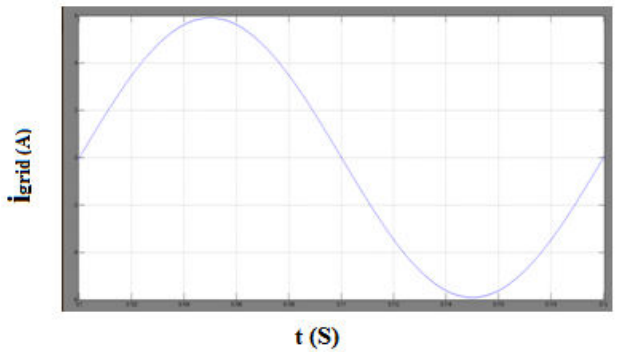

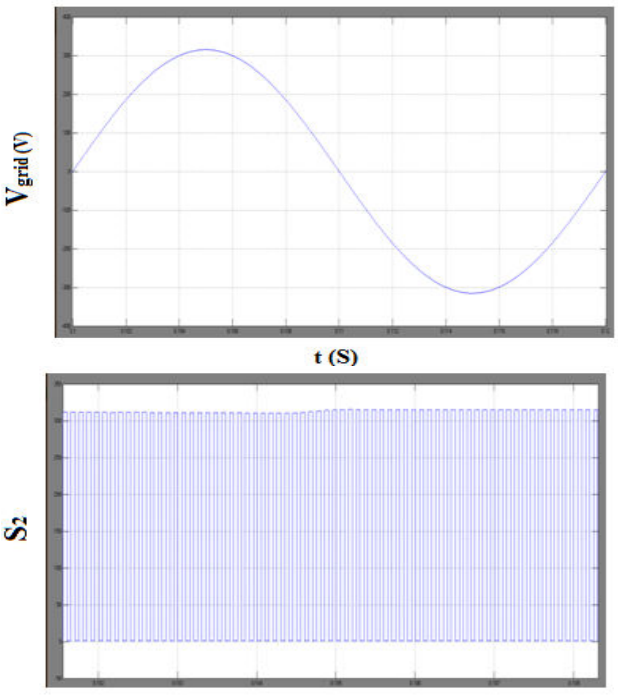

International Journal for Innovative Engineering and Management Research
A Peer Revieved Open Access International Journal
www.ijiemr.org

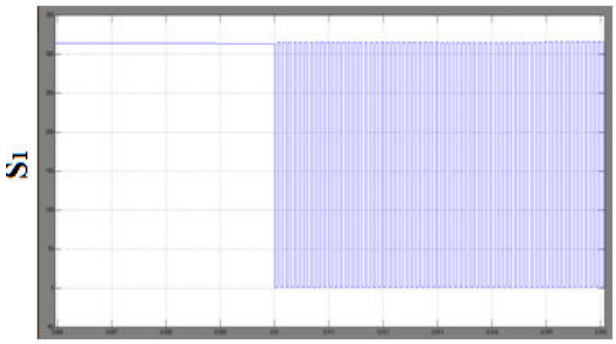

(a) Grid charging (mode 5)

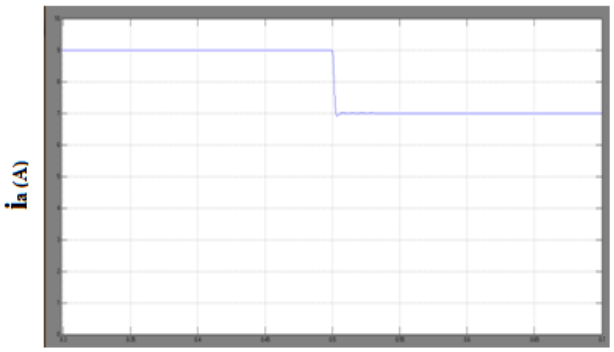

(b) PV charging mode 6 (stage 1 to stage 2)

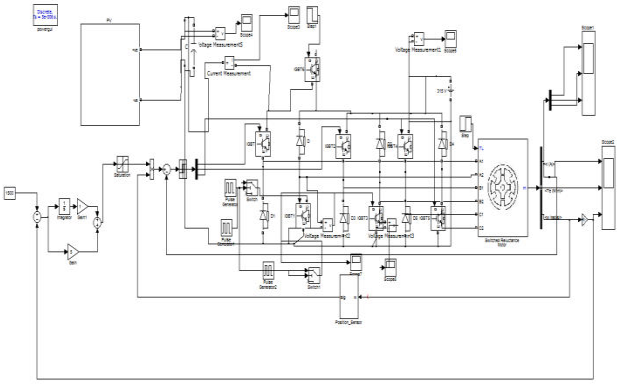

Fig.19 PV-powered SRM drive model diagram

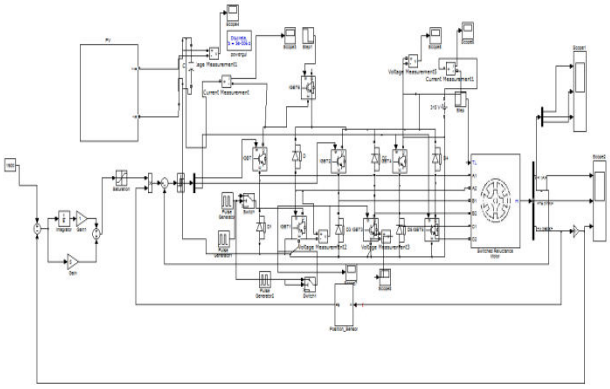

Fig.20 PV-powered SRM drive model diagram

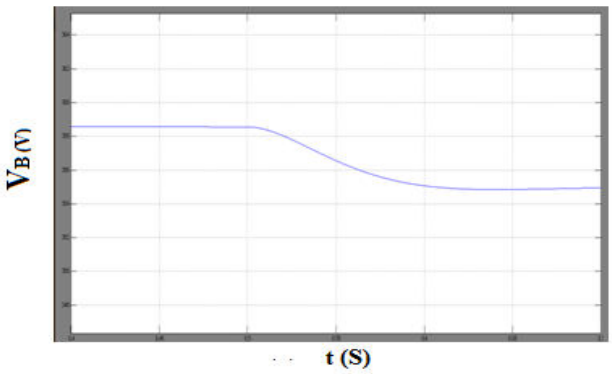

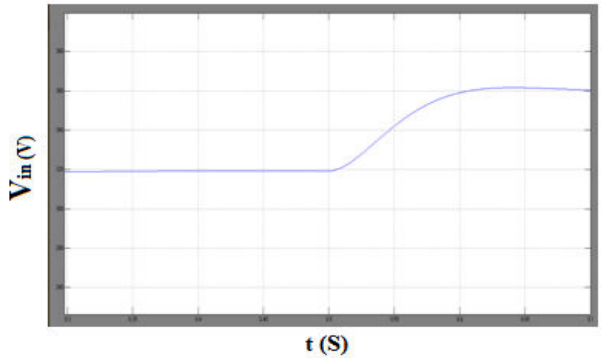

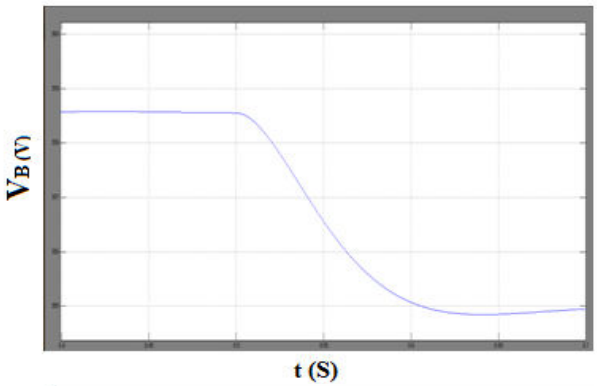

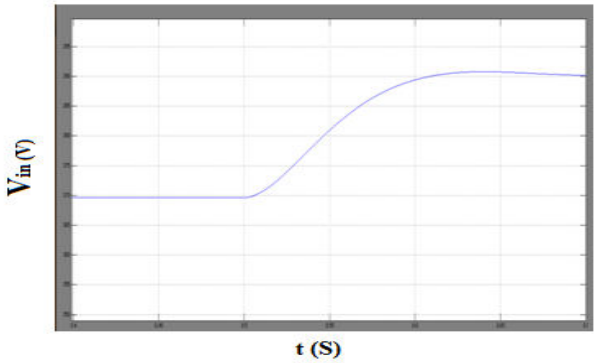

International Journal for Innovative Engineering and Management Research
A Peer Revieved Open Access International Journal
www.ijiemr.org

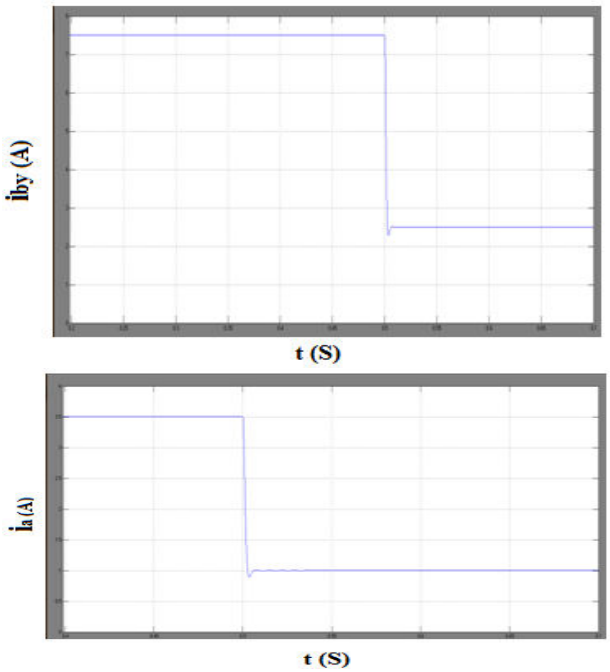

(c) PV charging mode 6 (stage 2 to stage 3)
Fig.21 simulation results for charging modes.

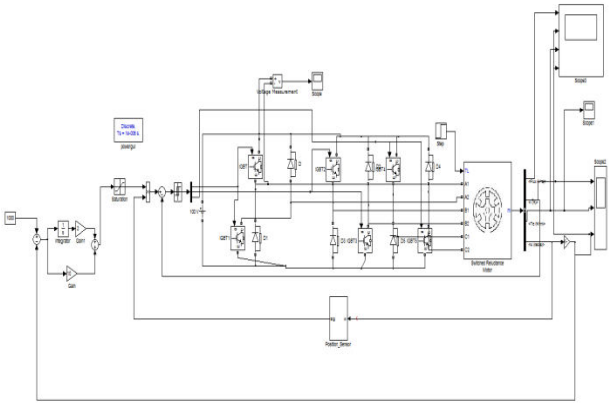

Fig.22 SRM drive model diagram With PI controller

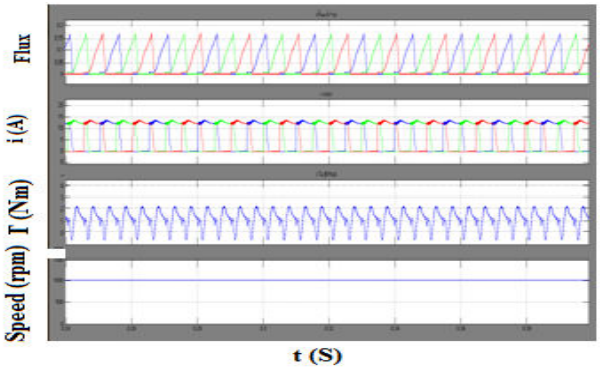

Fig.23 Flux, Current, Speed and Torque

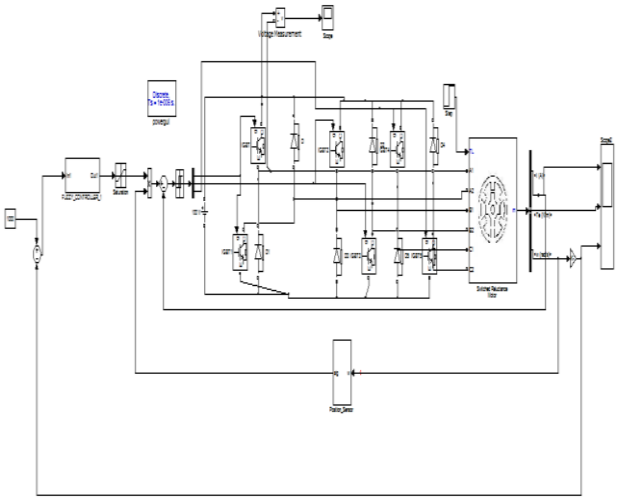

Fig.24 SRM drive model diagram With Fuzzy controller

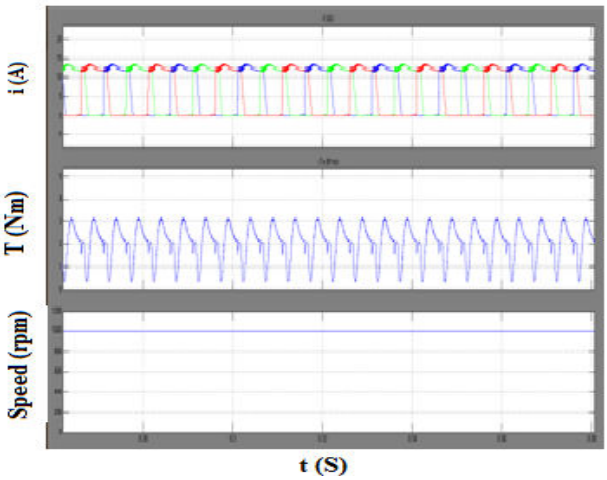

Fig.25 Current, Speed and Torque

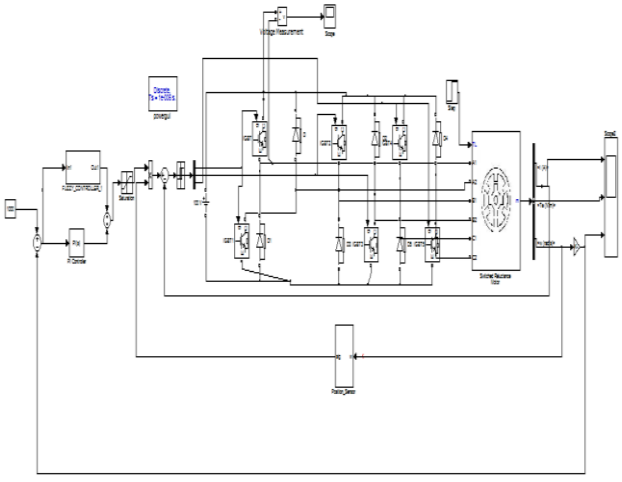

Fig.26 SRM drive model diagram With Hybrid Fuzzy controller

International Journal for Innovative Engineering and Management Research
A Peer Revieved Open Access International Journal
www.ijiemr.org

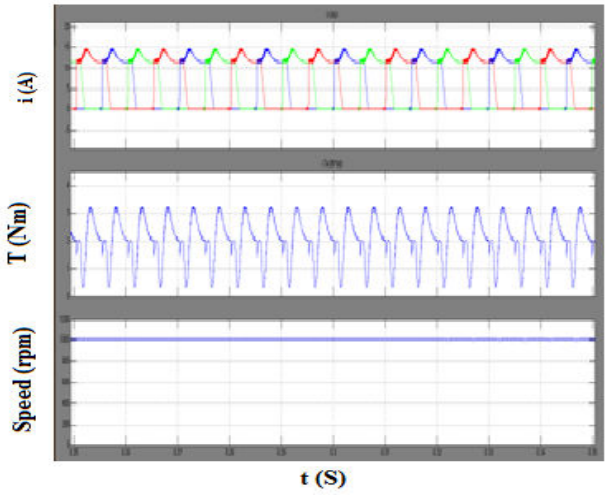

Fig.27 Current, Torque and Speed

VI. CONCLUSION

In this project in order to tackle the range anxiety of using EVs and decrease the system cost, a combination of the PV panel and SRM is proposed as the EV driving system. In this a tri-port converter is used to coordinate the PV panel, battery and SRM. Six working modes are developed to achieve flexible energy flow for driving control, driving/charging hybrid control and charging control. A novel grid-charging topology is formed without a need for external power electronics devices. A PV-fed battery charging control scheme is developed to improve the solar energy utilization. Since PV-fed EVs are a greener and more sustainable technology than conventional ICE vehicles, this work will provide a feasible solution to reducing the total costs and CO2emissions of electrified vehicles. It is shown that the presented hybrid controller for SRM drive has fast tracking capability, less steady state error and is robust to load disturbance. The complete speed control scheme of the SRM drive incorporating the hybrid control was implemented. From the above results it is clearly observed that the proposed controller despite of its simple structure has good speed response, high precision speed controller (Hybrid fuzzy) for operating in the whole of speed range and for any loading and environmental conditions were achieved.

REFERENCES

[1] A. Emadi, L. Young-Joo, K. Rajashekara, "Power electronics and motor drives in electric, hybrid electric, and plug-in hybrid electric vehicles," IEEE Trans. Ind. Electron., vol. 55, no. 6, pp. 2237-2245, Jun. 2008.

[2] B. l. K. Bose, "Global energy scenario and impact of power electronics in21st century," IEEE Trans. Ind. Electron., vol. 60, no. 7, pp. 2638-2651,Jul. 2013.

[3] J. de Santiago, H. Bernhoff, B. Ekergård, S. Eriksson, S. Ferhatovic, R. Waters, and M. Leijon, "Electrical motor drivelines in commercial all electric vehicles: a review," IEEE Trans. Veh. Technol., vol. 61, no. 2, pp. 475-484, Feb. 2012.

[4] Z. Amjadi, S. S. Williamson, "Power-electronics-based solutions for plug in hybrid electric vehicle energy storage and management systems," IEEE Trans. Ind. Electron., vol. 57, no. 2, pp. 608-616, Feb. 2010.

[5] A. Kuperman, U. Levy, J. Goren, A. Zafransky, and A. Savernin, "Battery charger for electric vehicle traction battery switch station," IEEE Trans. Ind. Electron., vol. 60, no. 12, pp. 5391-5399, Dec. 2013.

[6] S. G. Li, S. M. Sharkh, F. C. Walsh, and C. N. Zhang, "Energy and battery management of a plug-in series hybrid electric vehicle using fuzzy logic," IEEE Trans. Veh. Technol., vol. 60, no. 8, pp. 3571-3585, Oct. 2011.

[7] C. H. Kim, M. Y. Kim, and G. W. Moon, "A modularized charge equalizer using a battery monitoring IC for series-connected Li-Ion battery Strings in electric vehicles," IEEE Trans. Power Electron., vol. 28, no. 8,pp. 3779-3787, May 2013.

[8] Z. Ping, Z. Jing, L. Ranran, T. Chengde, W. Qian, "Magnetic characteristics investigation of an axial-axial flux compound-structure PMSM used for HEVs," IEEE Trans. Magnetics, vol. 46, no. 6, pp. 2191-2194, Jun. 2010.
[9] A. Kolli, O. Béthoux, A. De Bernardinis, E. Labouré, and G. Coquery, "Space-vector PWM control synthesis for an H-bridge drive in electric vehicles," IEEE Trans. Veh. Technol., vol.62, no.6, pp. 2441-2452, Jul.2013.
[10] http://www. Blue-birdelectric. Net / blue planet _ eco star / solar_assisted_electric_vehicles_sustainable_transport_cars_vans.htm
[11] S. M. Yang, and J. Y. Chen, "Controlled dynamic braking for switched reluctance motor drives with a rectifier front end," IEEE Trans. Ind. Electron., vol. 60, no. 11, pp. 4913- 4919, Nov. 2013.
[12] B. Bilgin, A. Emadi, M. Krishnamurthy, "Comprehensive evaluation of the dynamic performance of a 6/10 SRM for traction application in PHEVs," IEEE Trans. Ind. Electron., vol. 60, no. 7, pp. 2564-2575, July.2013.
[13] M. Takeno, A. Chiba, N. Hoshi, S. Ogasawara, M. Takemoto, M. A. Rahman, "Test results and torque improvement of the 50-kW switched reluctance motor designed for hybrid electric vehicles," IEEE Trans. Ind. Appl., vol. 48, no. 4, pp. 1327-1334, Jul/Aug. 2012.
[14] A. Chiba, M. Takeno, N. Hoshi, M. Takemoto, S. Ogasawara, M. A. Rahman, "Consideration of number of series turns in switched-reluctance traction motor competitive to HEV IPMSM," IEEE Trans. Ind. Appl., vol.48, no. 6, pp. 2333-2340, Nov/Dec. 2012.
[15] I. Boldea, L. N. Tutelea, L. Parsa, and D. Dorrell, "Automotive electric propulsion systems with reduced or no permanent magnets: an overview," IEEE Trans. Ind. Electron., vol. 60, no. 9, pp. 5696- 5710, Oct. 2014.